

Formation mechanisms of tripod and tetrapod CdTe_{0.67}Se_{0.33} nanocrystals

X. H. Liu¹, C. Wang², X. F. Duan³, Y. Q. Wang^{2,*}, G. J. Liu², F. Y. Diao², P. Yang⁴, and J. P. Zhang^{1,*}

Received 29 April 2016, accepted 27 May 2016

Published online 25 July 2016

CdTe_{0.67}Se_{0.33} nanocrystals were synthesized using a typical organic route. Two major morphologies are observed from transmission electron microscopy (TEM) images, one being a tripod, and the other being a tripod-like with a black dot in the center of the nanocrystal. The nanocrystals have two distinct geometrical shapes, one being a tripod, and the other being a tetrapod. High-resolution TEM (HRTEM) examinations show that the tetrapod nanocrystals consist of a zinc-blende nucleus and four wurtzite arms connected through a common facet, whereas the tripod nanocrystals result from the coalescence of three zinc-blende nanorods. These results are helpful to interpret the growth process of other II–VI semiconductor NCs.

1 Introduction

Colloidal semiconductor nanoparticles have been extensively studied as active components in a variety of basic research and technological applications owing to their unique and superior optical, electrical, and magnetic properties [1] and potential application in lasers [2], light-emitting diodes [3], biological labels [4], and solar cells [5]. The size and shape of semiconductor nanocrystals (NCs) play an important role in determining their physical and chemical properties. During the past few years much effort has been devoted to preparing nanostructured materials with different morphologies such as nanowires, nanotubes, nanobelts, nanorings, nanosprings, nanocombs, and zigzags [6–11]. The synthesis of complex nanostructures, especially well-defined three-dimensional (3D) nanoarchitectures, makes the 3D functional materials and devices possible. The tetrapod-shaped NCs present a variety of promising mechanical, optical, and electrical properties. For example, due to their 3D character, tetrapods can contribute to the mechanical reinforcement of polymers as

additives. Since Alivisatos and co-workers successfully synthesized tetrapod-shaped CdSe NCs by thermal decomposition of organometallic precursors [12], other researchers have fabricated a variety of tetrapod-shaped II–VI semiconductor NCs including ZnSe, CdTe, CdS, CdSe, CdTe_xSe_{1-x} and ZnO [13–19].

Up to now, there is still controversy over the growth mechanism of tetrapod-shaped NCs. Takeuchi et al. [20] proposed a wurtzite octahedral multiple twin nucleus model for the tetrapod-shaped ZnO particles. Gong et al. [21] showed direct evidence of a zinc-blende octahedron nucleus model for the ZnS tetrapods, which is consistent with the tetrapod CdTe crystals [14]. Zhang et al. [17] thought that the tetrapodal CdTe_{0.67}Se_{0.33} NCs consist of a zinc-blende tetrahedral core and four wurtzite branches. Therefore, it is necessary to clarify the growth mechanism of the tetrapod-shaped NCs.

In this paper, we report on the morphological and microstructural investigations of the CdTe_{0.67}Se_{0.33} NCs using scanning transmission electron microscopy (STEM) and high-resolution transmission electron microscopy (HRTEM). It is found that they have two main geometrical shapes, one being a tripod, and the other being

* Corresponding authors: e-mail: jpzhang2008@sinano.ac.cn, Tel. no.: +86-512-62872601
yqwang@qdu.edu.cn, Tel. no.: +86-532-83780318

¹ Platform for Characterization and Test, Institute of Nano-tech and Nano-bionics, Chinese Academy of Sciences, Suzhou, 215123 People's Republic of China

² College of Physics & The Cultivation Base for State Key Laboratory, Qingdao University, No. 308 Ningxia Road, Qingdao 266071, People's Republic of China

³ Laboratory of Advanced Materials and Electron Microscopy, Institute of Physics, Chinese Academy of Sciences, Beijing 100080, People's Republic of China

⁴ School of Materials Science and Engineering, University of Jinan, Jinan 250022, People's Republic of China

a tetrapod. Their growth mechanisms are also clarified, which are helpful to interpret the growth process of other II–VI semiconductor NCs.

2 Experimental section

$\text{CdTe}_{0.67}\text{Se}_{0.33}$ NCs were prepared by a typical low-cost, facile organic route. [17] Te and Se mixture with a molar ratio of 0.67 was dissolved in trioctylphosphine (TOP) solution. 30 mg of cadmium oxide (CdO), 1 g of stearic acid (SA), and 5 mL of 1-octadecene in a three-necked flask were heated to 150 °C under rapid stirring and degassing by N_2 . The flask was heated until CdO was dissolved completely, and then a clear solution of CdO was produced at 240 °C. Finally, the temperature was further increased up to 260 °C under N_2 flow and was maintained for 2 min, and 0.5 mL of TOPSe and TOPTe mixtures were injected into the solution with a speed of 1 mL/min.

Selected-area electron diffraction (SAED) and HRTEM examinations were carried out using a Philips CM200-FEG transmission electron microscope operating at 200 kV, and the high-angle annular dark field (HAADF) observations were carried out using a Tecnai G2 F20 S-TWIN scanning transmission electron microscope (STEM) operating at 200 kV.

3 Results and discussion

Figure 1(a) is a low-magnification TEM image of NCs. It can be clearly seen from figure 1(a) that the $\text{CdTe}_{0.67}\text{Se}_{0.33}$ NCs have two different morphologies, one being a tripod (labeled by I), and the other being a tripod-like with a black dot in the central position of the nanocrystal (labeled by II). The SAED pattern in the inset of figure 1(a) demonstrates that these particles have a typical zinc-blende structure with characteristic (111), (220), and (311) diffraction rings. Figure 1(b) shows typical HAADF images of the branched $\text{CdTe}_{0.67}\text{Se}_{0.33}$ NCs when α angle of the specimen holder is 0°. It can be clearly seen from figure 1(b) that the branched $\text{CdTe}_{0.67}\text{Se}_{0.33}$ NCs have two different morphologies, one being a tripod (labeled by A_1), and the other being a tripod-like (labeled by B_1) with a much brighter core. The brighter core in the tripod-like nanocrystal can be produced either by a higher atomic number element or thicker sample. Figure 1(c) shows typical HAADF images of the branched $\text{CdTe}_{0.67}\text{Se}_{0.33}$ NCs when the specimen is tilted to 25°. It can be clearly seen from figure 1(c) that after tilting the specimen, the brighter core in figure 1(b) turns into the fourth branch of the NCs

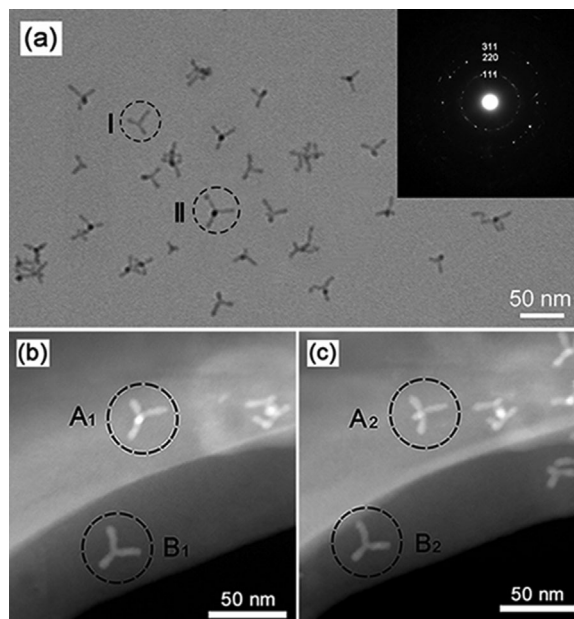


Fig. 1 (a) TEM images of the branched $\text{CdTe}_{0.67}\text{Se}_{0.33}$ NCs with Te/Se molar ratio of 0.67, the corresponding SAED; Typical HAADF images of the $\text{CdTe}_{0.67}\text{Se}_{0.33}$ NCs: (b) $\alpha = 0^\circ$; (c) $\alpha = 25^\circ$.

(labeled by A_2) which confirms that the thickness is the dominant reason for the brighter core, and the tripod NCs without a much brighter core (labeled by B_1) in figure 1(b) do not change after tilting the specimen (demonstrated by B_2 in figure 1(c)). Therefore, we can draw a conclusion that the $\text{CdTe}_{0.67}\text{Se}_{0.33}$ NCs have two different morphologies, tripod and tetrapod. In the tetrapod $\text{CdTe}_{0.67}\text{Se}_{0.33}$ NCs, three branches are stretched out on a copper grid and one branch extends upward to reveal a triangle-like branched structure in figure 1(b), and the fourth branch overlaps with the core resulting in a much brighter core (labeled by A_2). In the literature [22, 23], both morphologies were observed in CdSe, CdTe, $\text{CdSe}_x\text{Te}_{1-x}$ NCs. However, they were regarded as tetrapod, which is different from our observation.

To clarify the growth mechanisms of these NCs, extensive HRTEM examinations were carried out. Figure 2(a) shows a typical HRTEM image of tetrapod $\text{CdTe}_{0.67}\text{Se}_{0.33}$ NCs formed by a core and four branches. It can be clearly seen from figure 2(a) that the angle between any two branches is 120°, while the fourth one overlaps with the core. From our HRTEM observations, four branches of the $\text{CdTe}_{0.67}\text{Se}_{0.33}$ NCs belong to the wurtzite phase and the core has a zinc-blende phase, consistent with the XRD result [17]. All the hexagonal branches are connected to the zinc-blende core along the four $\langle 111 \rangle$ directions and the growth facets of the four hexagonal branches are $\{0001\}$. Because the

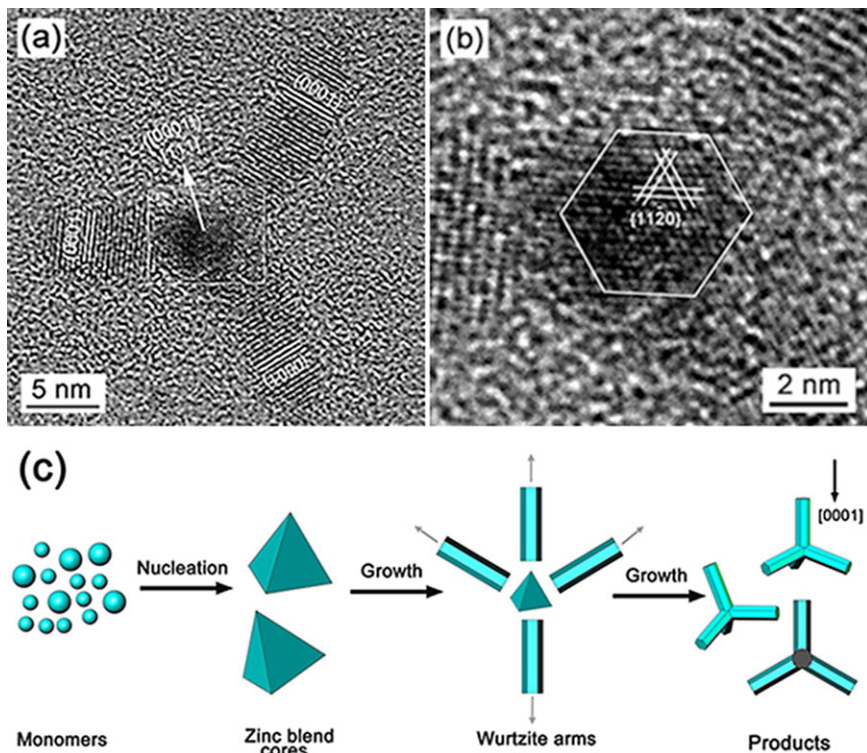


Fig. 2 (a) HRTEM image of the tetrapod $\text{CdTe}_{0.67}\text{Se}_{0.33}$ nanocrystal; (b) Enlarged HRTEM image of the core region; (c) Schematic diagram of formation mechanism.

{111} facets of the zinc-blende structure are atomically identical to {0001} facets of the wurtzite structure, the fourth branch overlaps with the core resulting in an imaging contrast which is shown in the center of the nanocrystal in figure 2(a). Meanwhile, it can be clearly seen from figure 2(a) that the three branches distributed at an angle of 120° to each other are uniform, and the zone-axis of them is $[1\bar{1}00]$. The zinc-blende octahedron nucleus model, which agrees well with the proposed structure model for the tetrapod CdTe crystals[14], could account for our experimental results. To show the atomic arrangements more clearly, an enlarged HRTEM image of the core is shown in figure 2(b), which is taken from the region enclosed by a rectangle in figure 2(a). It can be clearly seen from figure 2(b) that the marked facets are $\{11\bar{2}0\}$ and the shape of the central part is a hexagon, illustrating the zone axis of the core is $[0001]$. Figure 2(c) shows a schematic diagram of the formation mechanism for the tetrapod NCs. As many researchers reported, a widely-accepted growth mechanism of tetrapodal NCs is a zinc-blende nucleation occurring at an early stage, followed by four wurtzite-phase branches which grow along their c axes on four (111) surface facets. The growth facets of the four hexagonal branches are $\{0001\}$.

Figure 3(a) shows the typical HRTEM image of the tripod $\text{CdTe}_{0.67}\text{Se}_{0.33}$ NCs. It can be clearly seen from figure 3(a) that the marked facets are $\{111\}$, illustrating

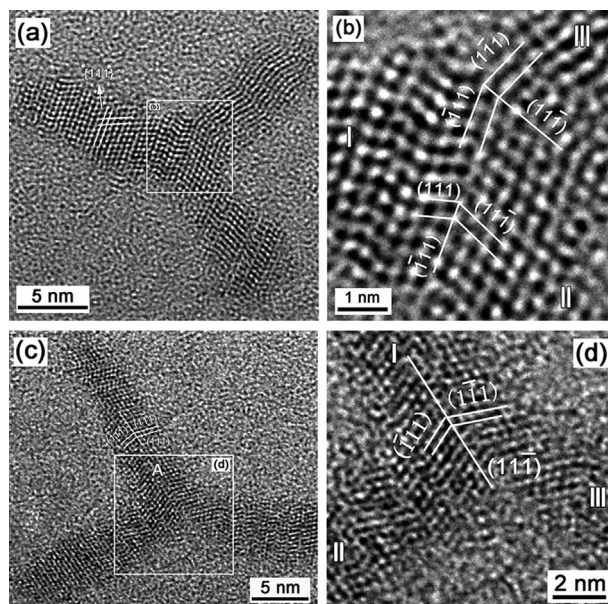


Fig. 3 HRTEM image of two different tripod $\text{CdTe}_{0.67}\text{Se}_{0.33}$ nanocrystals: (a) and (c); (b) and (d) Enlarged HRTEM image of the region enclosed by a rectangle in (a) and (c).

ing the tripod $\text{CdTe}_{0.67}\text{Se}_{0.33}$ NCs have zinc-blende phase. Figure 3(b) is the enlarged HRTEM image of the region enclosed by a rectangle in (a). It can be clearly seen from figure 3(b) that two nanocrystal groups are connected

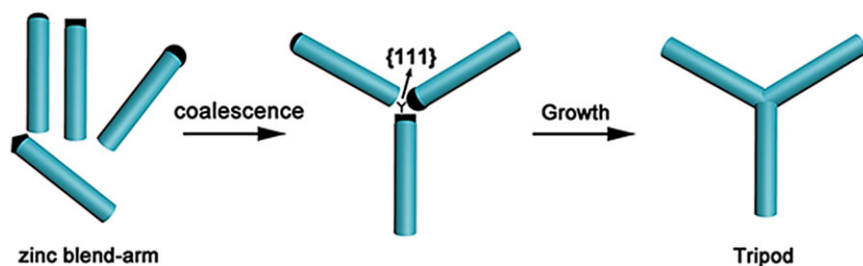


Fig. 4 Schematic diagram of the formation mechanism for CdTe_{0.67}Se_{0.33} tripod NCs.

with each other by forming a twin and the twin boundary is defined as $\{111\}$. Figure 3(c) shows the typical HRTEM image of another tripod CdTe_{0.67}Se_{0.33} nanocrystal. It can be seen that one branch of the tripod nanocrystal (labeled by A) is a twin crystal and the two domains of the twin crystal share the $(11\bar{1})$ twin boundary. Similarly, this tripod CdTe_{0.67}Se_{0.33} nanocrystal also has a zinc-blende structure which illustrates the nanocrystal does not derive from the broken tetrapod one. It can be clearly seen from figure 3(d) that two branches (labeled by II and III) are connected to the other one (labeled by I) and their growth facets are $\{111\}$. From the results, we can see that the three-branch is a remarkable feature of the CdTe_{0.67}Se_{0.33} NCs.

From the above analysis, a growth model is proposed which is shown in figure 4. Firstly, a core with irregular shape forms followed by a nanorod. Three nanorods with $\{111\}$ facets coalesce into a tripod nanocrystal by twinning. The coalescence behavior of the nanorods is determined by the position of $\{111\}$ facets. HRTEM images similar to figures 3(a) and 3(b) were reported in the literatures [22, 23] and the authors thought the HRTEM images were taken along one direction of the core where two arms overlapped to each other. However, these explanations could not account for our experiment results.

4 Conclusions

In summary, STEM and HRTEM examinations demonstrate that the CdTe_{0.67}Se_{0.33} NCs have two distinct geometrical shapes, one being a tetrapod with a zinc-blende tetrahedral core and four wurtzite branches growing out from the core along its four $\langle 111 \rangle$ directions, and the other being a tripod formed by coalescence of three zinc-blende branches which are related to each other by the $\{111\}$ twins.

Acknowledgements. The authors would like to acknowledge the financial support from National Key Basic Research Development Program of China (Grant no.: 2012CB722705), the Natural Science Foundation for Outstanding Young Scientists in Shandong Province (Grant No.: JQ201002), and High-end Foreign

Experts Recruitment Program (Grant nos.: GDW20133400112, GDW20143500163). Y. Q. Wang would also like to thank the financial support from Top-notch Innovative Talent Program of Qingdao City (13-CX-8), and Taishan Outstanding Overseas Scholar Program of Shandong Province.

Key words. CdTe_{0.67}Se_{0.33} nanocrystals, Tetrapod and tripod, Formation mechanism.

References

- [1] Y. H. Leung, W. M. Kwok, A. B. Djurić, D. L. Phillips, and W. K. Chan, *Nanotechnology* **16**, 579 (2005).
- [2] N. Tessler, V. Medvedev, M. Kazes, S. H. Kan, U. Banin, *Science* **295**, 1506 (2002).
- [3] M. C. Schlamp, X. Peng, and A. P. Alivisatos, *J. Appl. Phys* **82**, 5837 (1997).
- [4] M. Bruchez, M. Moronne, P. Gin, S. Weiss, and A. P. Alivisatos, *Science* **281**, 1203 (1998).
- [5] W. Huynh, X. Peng, and A. P. Alivisatos, *Adv. Mater* **11**, 923 (1999).
- [6] M. Law, J. Goldberger, and P. Yang, *Annu. Rev. Mater. Sci.* **34**, 83 (2004).
- [7] Z. L. Wang, *Rev. Phys. Chem.* **55**, 159 (2004).
- [8] X. Y. Kong, Y. Ding, R. Yang, and Z. L. Wang, *Science* **303**, 1348 (2004).
- [9] X. Y. Kong, and Z. L. Wang, *Nano Lett* **12**, 1625 (2003).
- [10] Z. L. Wang, X. Y. Kong, and J. M. Zuo, *Phys. Rev. Lett.* **91**, 185502 (2003).
- [11] J. H. Duan, S. G. Yang, H. W. Liu, J. F. Gong, H. B. Huang, X. N. Zhao, R. Zhang, and Y. W. Du, *J. Am. Chem. Soc* **127**, 6180 (2005).
- [12] L. Manna, E. C. Scher, and A. P. Alivisatos, *J. Am. Chem. Soc* **122**, 12700 (2000).
- [13] P. D. Cozzoli, L. Manna, M. L. Curri, S. Kudera, C. Gianini, M. Striccoli, and A. Agostiano, *Chem. Mater.* **17**, 1296 (2005).
- [14] L. Manna, D. J. Milliron, A. Meisel, E. C. Scher, and A. P. Alivisatos, *Nat. Mater.* **2**, 902 (2003).
- [15] F. Gao, Q. Y. Lu, S. H. Xie, D. Y. Zhao, *Adv. Mater* **14**, 1537 (2002).
- [16] L. Manna, E. C. Scher, and A. P. Alivisatos, *J. Am. Chem. Soc.* **122**, 12700 (2000).
- [17] R. L. Zhang, and P. Yang, *J. Nanopart. Res.* **14**, 1083 (2012).

- [18] Q. H. Li, Q. Wan, Y. J. Chen, T. H. Wang, H. B. Jia, and D. P. Yu, *Appl. Phys. Lett.* **85**, 636 (2004).
- [19] Y. Dai, Y. Zhang, and Z. L. Wang, *Solid State Commun.* **126**, 629 (2003).
- [20] S. Takeuchi, H. Iwanaga, and M. Fujii, *Philos. Mag. A* **69**, 1125 (1994).
- [21] J. F. Gong, and S. G. Yang, *Small* **2**, 732 (2006).
- [22] Q. Pang, L. J. Zhao, Y. Cai, D. P. Nguyen, N. Regnault, N. Wang, S. H. Yang, W. K. Ge, R. Ferreira, G. Bastard, and J. N. Wang, *Chem. Mater.* **17**, 5263 (2005).
- [23] Y. C. Li, H. Z. Zhong, R. Li, Y. Zhou, C. H. Yang, and Y. F. Li, *Adv. Funct. Mater.* **16**, 1705 (2006).